A Journal of the Gesellschaft Deutscher Chemiker
Angewandte Chemie
International Edition
www.angewandte.org

Accepted Article

Title: Subnanocatalysis for Aerobic Oxidation: Toluene Oxidation with Oxygen using Subnano Metal Particles

Authors: Kimihisa Yamamoto, Miftakhul Huda, Keigo Minamisawa, Takamasa Tsukamoto, and Makoto Tanabe

To be cited as: *Angew. Chem. Int. Ed.* 10.1002/anie.201809530
Angew. Chem. 10.1002/ange.201809530

Link to VoR: http://dx.doi.org/10.1002/anie.201809530
http://dx.doi.org/10.1002/ange.201809530

WILEY-VCH

10.1002/anie.201809530

Aerobic Toluene Oxidation Catalyzed by Subnano Metal Particles

Miftakhul Huda,[a,b] Keigo Minamisawa,[a] Takamasa Tsukamoto,[a,b] Makoto Tanabe,*[a,b] and Kimihisa Yamamoto*[a,b]

Abstract: Subnanocatalysts (SNCs) containing various noble metals (Cu, Ru, Rh, Pd, or Pt) with sizes of approximately 1 nm were synthesized using dendritic poly(phenylazomethine)s as a macromolecular template. These materials exhibit high catalytic performance during toluene oxidation without the use of harmful solvents or explosive oxidants, resulting in the formation of valuable organic products, including benzoic acid as the major product. In particular, Pt_{19} SNC with a narrow particle size distribution exhibits extraordinary catalytic activity, with a turnover frequency of 3238 atom^{-1} h^{-1}, which is 1700 times greater than that obtained by commercial Pt/C catalysts.

Catalytic oxidation of hydrocarbons is a critically important process that converts raw materials into versatile organic compounds.[1] However, the majority of the practices currently employed in industry suffer from several disadvantages, such as the use of oxidants hazardous to the environment, poor selectivity, and excessive waste generation. Applying molecular oxygen as the oxidant in conjunction with solvent-free reaction systems has attracted considerable attention as a benign, inexpensive approach to catalytic oxidations.[2] For this reason, many researchers have studied nanometer-sized heterogeneous catalysts. However, decreasing the size of the catalyst to the subnanometer scale would further reduce the quantities of noble metals required for catalysis. The catalytic properties of subnanocatalysts (SNCs) with sizes of approximately 1 nm have been investigated because the lattice structure normally found in nanoparticles is collapsed in such materials and they exhibit quantum size effects as a result of the amorphous surface areas and the irregular electron distributions.[3] In addition, noble metal SNCs are resistant to oxidation even under an oxygen atmosphere. As an example, noble metal SNCs composed of Rh,[4] Pd,[5] Pt,[6] and Au[7] exhibit highly effective and selective catalysis during CO oxidation. Size-specific Pt SNCs were also found to be more active for the dehydrogenation of propane than larger nanocatalysts.[8] However, the precise synthesis of such particles while controlling the quantity of metallic atoms per particle is remarkably difficult.

[a] Dr. M. Huda, K. Minamisawa, Dr. T. Tsukamoto, Dr. M. Tanabe, Prof. Dr. K. Yamamoto
Institute of Innovative Research, Tokyo Institute of Technology
4259 Nagatsuta, Midori-ku, Yokohama 226-8503 (Japan)
E-mail: yamamoto@res.titech.ac.jp,
[b] JST–ERATO, Yamamoto Atom Hybrid Project, Tokyo Institute of Technology, 4259 Nagatsuta, Midori-ku, Yokohama 226-8503 (Japan).

Supporting information for this article is given via a link at the end of the document.

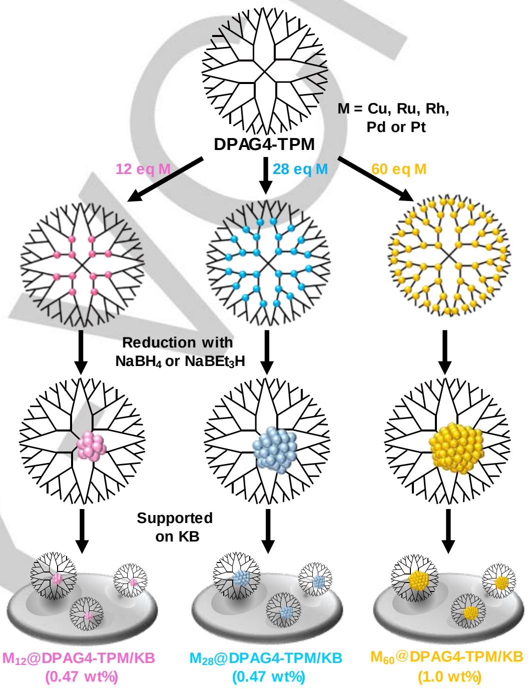

Figure 1. Schematic representation to prepare heterogeneous transition-metal SNCs M_n@DPA G4/KB (M = Cu, Ru, Rh, Pd, and Pt, n = 12, 28, and 60, KB = Ketjenblack).

The dendrimer-templated method is an effective strategy for the synthesis of size-controlled subnano metal particles in conjunction with low polydispersity.[9] Dendrimers provide internal nanospaces that could be suitable for catalytic conversion in the presence of metal particles.[10] Our group has prepared subnano platinum particles with atomic-level precision using fourth-generation dendritic poly(phenylazomethine) species having a tetraphenylmethane core (DPAG4-TPM) or a mono(2-pyridyl)-triphenylmethane core (DPAG4-PyTPM).[11] A prior electrochemical study found that SNCs containing between 12 and 20 Pt atoms exhibit superior catalytic performance.[12] In other work, multi-metal alloy nanocatalysts containing Au, Pt, and Cu atoms showed enhanced catalytic activity during solvent-free aerobic oxidation of hydrocarbons with secondary C–H bonds.[13] In contrast, a similar oxidation of the primary C–H bonds of toluene normally requires harsh conditions, such as elevated temperatures and high oxygen pressures. Recently, Hutchings *et al.* reported that Au-Pd mixed nanocatalysts (> 3 nm) promoted toluene oxidation with oxygen to give benzyl benzoate as the main product.[14] However, these Au-Pd nanoparticles were found to form crystalline surfaces, resulting in low turnover numbers. Other conventional heterogeneous catalysts have to date exhibited poor catalytic performance during solvent-free toluene oxidation.[15] In

10.1002/anie.201809530

the present study, we demonstrated the preparation of a series of ultra-small noble metal SNCs and assessed the catalytic performance of these materials during toluene oxidation with oxygen, giving valuable organic compounds.

We synthesized precisely size-controlled SNCs containing Cu, Ru, Rh, Pd, or Pt atoms composed of 12, 28, or 60 atoms, using a DPAG4-TPM template method (Figure 1). The synthetic procedure employed was similar to a previously reported method.[11] Pt SNCs composed of the number between 12 and 28 were also synthesized using DPAG4-PyTPM as the template to obtain a narrower size distribution.[12c] Novel Ru, Rh, and Pd SNCs were prepared via the stepwise titration of $RuCl_3$, $RhCl_3$, or $[Pd(MeCN)_4](BF_4)_2$ in the appropriate solvents followed by chemical reduction with an excess of $NaBH_4$ or $NaBEt_3H$. All SNCs were supported on carbon (Ketjenblack: KB) for use as heterogeneous catalysts, with estimated loadings of 0.47 wt% for M_{12} to M_{28} and 1.0 wt% for M_{60}.

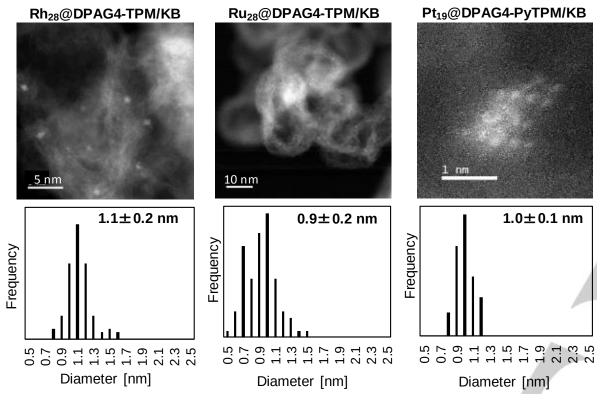

Figure 2. HAADF-STEM images (80 kV) of Ru_{28} and Rh_{28} SNCs and histograms of the particle-size distributions, and atomic resolution HAADF-STEM image of Pt_{19} SNC prepared by a DPAG4-PyTPM template.

High-angle annular dark-field scanning transmission electron microscopy (HAADF-STEM) images of subnano Ru_{28} and Rh_{28} particles on KB showed SNCs with mean diameters of 0.9 and 1.1 nm with a narrow size distribution of ±0.2 nm, respectively (Figure 2). The formation of Pt_{19} SNCs (1.0±0.1 nm) via the DPAG4-PyTPM template was confirmed by atomic resolution HAADF-STEM image as a representative particle. X-ray photoelectron spectroscopy (XPS, Figures S9-S11) data acquired from subnano Pt_{60} particles showed a peak at 71.6 eV (corresponding to Pt $4f_{7/2}$) that suggested that the Pt was in a zero-valent oxidation state.[12a] Two signals were generated by the subnano Rh and Pd particles (Rh $3d_{5/2}$: 307.5 and 309.5 eV, Pd $3d_{5/2}$: 335.9 and 337.0 eV), indicating two different electronic states in both cases. These were assigned to Rh(0) and Pd(0) and to the metals in their oxidized states, respectively, due to partial oxidation at the surface by reaction with atmospheric oxygen.[16] Binding energies of 463.0 eV were observed for Ru $3p_{5/2}$,[17] and 932.9 and 934.0 eV for Cu $2p_{3/2}$,[18] which demonstrated the presence of RuO_2 (Ru $3p_{3/2}$: 462.3 eV) and CuO (Cu $3p_{5/2}$: 933.7 eV). These oxophilic subnano metal particles were readily oxidized by reaction with oxygen molecules as a result of their larger surface areas and lower electron densities relative to the bulk materials.

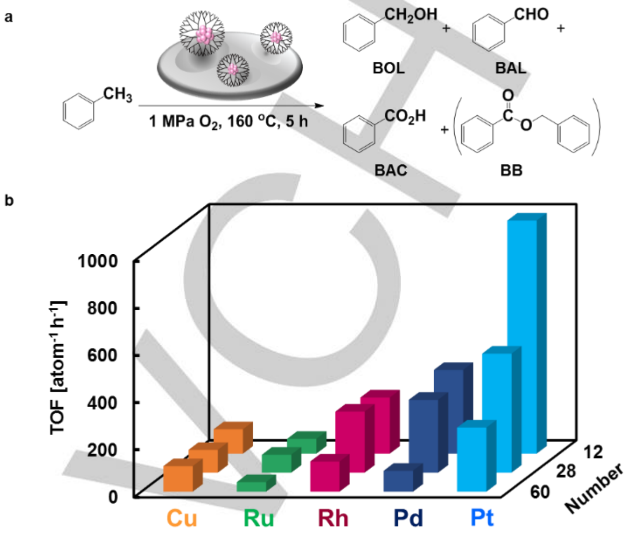

c

TOF		Cu_{28}	Ru_{28}	Rh_{28}	Pd_{28}	Pt_{28}
	BOL	29	15	59	67	120
	BAL	31	43	72	82	123
	BAC	35	18	125	153	222
	BB	0	1	3	6	4
	Total	96	76	259	308	469

Figure 3. Toluene oxidation with oxygen catalysed by noble metal SNCs. **a** These SNCs were synthesized using a DPAG4-TPM template. The catalytic reactions were performed at 160 °C under 1 MPa oxygen for 5 h. **b** Total TOFs calculated from the sum of the TOFs for each product. All TOFs were evaluated on the basis of the estimated metal loading amount of 0.47 wt% for M_{12} to M_{28} and 1.0 wt% for M_{60}. **c** The TOFs for each product catalysed by subnano M_{28} particles: BOL = benzyl alcohol, BAL = benzaldehyde, BAC = benzoic acid, BB = benzyl benzoate.

After characterization of the noble metal SNCs, catalytic toluene oxidation trials were carried out under an oxygen atmosphere (1 MPa) at 160 °C in a stainless autoclave for 5 h. These catalytic reactions provided a mixture of benzyl alcohol, benzaldehyde, and benzoic acid as the major products, while the amount of benzyl benzoate was almost negligible. The catalytic activities of the SNCs having 12, 28, or 60 and Cu, Ru, Rh, Pd, or Pt atoms were estimated from the sums of the turnover frequency (TOF) values for each of the oxidized products (Figure 3). Control experiments without any subnano metal particles on the KB support under the same conditions did not show any catalytic activity. In addition, a trial was performed in which the Pt loading on the KB support was increased, using Pt_{28} SNC (Figure S14). The total product yield was increased as the Pt loading increased to 1.4 wt% based on the mass of the KB support. This increase in yield relative to the mass of the Pt SNCs confirms the catalytic activity of the SNCs for the toluene oxidation, presumably through the activation of oxygen on the SNC surfaces. The oxidized subnano Cu_{28} or Ru_{28} particles identified by XPS spectroscopy showed low catalytic activity, with TOF values of 96 and 76 atom^{-1} h^{-1}, respectively, while the partially oxidized subnano Rh_{28} (259 atom^{-1} h^{-1}) and Pd_{28} (308 atom^{-1} h^{-1}) particles exhibited higher

10.1002/anie.201809530

activity. The less oxophilic subnano Pt_{28} particles (469 atom^{-1} h^{-1}) had the highest catalytic activity among these M_{28} particles. In addition, it was found that the catalytic activity of the Pt SNCs was dependent on the number of Pt atoms was decreased (Pt_{12}: 987 atom^{-1} h^{-1}, Pt_{60}: 271 atom^{-1} h^{-1}). The size-dependent catalytic activity is similar to that obtained from the Pt SNCs during electrochemical oxygen reduction.[12a] These results suggest that the catalytic performance of these materials is strongly related to the oxophilicity of the corresponding subnano metal particles as determined by the XPS analysis.

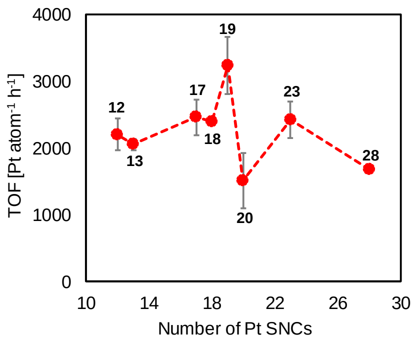

Figure 4. Catalytic performance of each Pt_n SNC during toluene oxidation. All Pt_n SNCs were synthesized by assembling complexation of $PtCl_4$ to a DPAG4-PyTPM template upon addition of the corresponding number of the metal halides. The catalytic reactions were performed at 160 °C under 1 MPa oxygen for 5 h. TOFs were calculated from the sum of the TOF for each product, on the basis of the actual metal amount determined from ICP-AES results (0.14-0.22 wt%).

The catalytic activity of the Pt SNCs from 12 to 28 atoms, prepared using the DPAG4-PyTPM template with estimated loadings of 0.47 wt%, were estimated as the range of the TOF values between 681 and 1064 atom^{-1} h^{-1} (Figure S15). When these TOF values were adjusted on the basis of the ICP-AES results for the actual Pt loadings (0.14-0.22 wt%, Table S1), the Pt_{19} SNCs exhibited the highest catalytic activity among the Pt_n SNCs (TOF: 3238 atom^{-1} h^{-1}, Figure 4). This superior activity is attributed to the presence of sites that allow the adsorption of oxygen with a low activation energy,[12c] or to a thermally stable geometry that maintains the catalyst structure at elevated temperatures.[19] The Pt_{19} cluster stabilized by CO ligands was reported to form a thermally stable double icosahedral structure.[20] In contrast, the larger size of Pt_{28} SNCs showed less catalytic activity (TOF: 1686 atom^{-1} h^{-1}). Furthermore, a commercially available Pt/carbon catalyst (10 wt% Pt/C) and Pt nanoparticles with an average size of 2.2 nm showed very low TOF values of 1.8 and 112 atom^{-1} h^{-1}, respectively. Similar results were obtained using commercially available Ru/C, Rh/C, and Pd/C catalysts (Figure S13). These results demonstrate the superior performance of the SNCs during toluene oxidation compared to the corresponding nanocatalysts. The catalytic activity of the Pt_{19} SNCs was 1700 times greater than those of commercially available Pt/C catalyst, respectively.

The mechanistic aspects of the catalytic transformation were investigated by an additional experiment using a radical scavenger, TEMPO (2,2,6,6-tetramethylpiperidine 1-oxyl), to inhibit the catalytic reaction. This trial provided evidence that the catalytic oxidation followed a radical-chain mechanism (Figure S18). Scheme 1 summarizes the plausible pathways for the activation of the molecular oxygen as catalyzed by the SNCs and by the larger nanoparticles. The former is significantly dependent on the oxophilicity of the transition metals. Nanocatalysts are capable of the adsorption of oxygen molecules with a side-on orientation on their surfaces and subsequent cleavage of the O–O bond via multi-electron transfer from the nanoparticles to the oxygen, resulting in the formation of the partial oxidation on the surface (Scheme 1a). The larger size of the nanoparticles (> 30 atoms) results in an electronic core-shell structure, with a positively charged core and a negatively charged shell.[21] The negatively charged surface possibly promotes charge transfer to the π^* orbital of the oxygen, similar to the mechanism that occurs on a metallic surface. The oxophilic SNCs such as Cu and Ru atoms lead to be reactive against molecular oxygen, resulting in the formation of the corresponding metal oxides (Scheme 1b-1). In contrast, the Pt SNCs could provide a superoxide radical species with an end-on coordination via a one-electron transfer from the electron-deficient particles (Scheme 1b-2). This radical species leads to a hydrogen abstraction transfer via the homolytic cleavage of the sp^3 hybridized C–H bonds of the toluene, followed by transformation between the hydroperoxide species on the surface and a tolyl radical to yield a toluene hydroperoxide intermediate. The SNCs consisting of less than 30 atoms exhibit a molecular like-nature because of their significantly highly active sites and lower electron densities, and so promote the end-on orientation of oxygen molecules.[22]

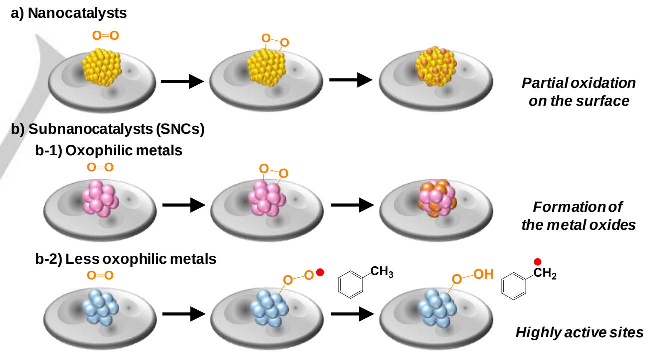

Scheme 1. Plausible mechanisms for activation of the molecular oxygen on the a) nanocatalysts and b) subnanocatalysts depending on the oxophilicity of the transition metals during the catalytic oxidations.

The reuse of these Pt SNCs for three replicate reactions resulted in a slight decrease in activity (Figure S22). The XPS analysis of Pt_{60} SNC after the reaction was shifted to high binding energy at 73.0 eV, indicating the partly oxidation state of the particle (Figure S26). This result would be attributed to the decrease of the reaction yield for the second run of reuse experiment. In addition, it is believed that the elevated temperature applied during the reaction may have detached the subnano platinum particles from the carbon support. For the catalytic reaction to proceed at room temperature, 1 mol% *tert*-butyl hydroperoxide (TBHP) was added, which gave rise to a very

10.1002/anie.201809530

slow reaction to give the same products after 195 h (Figure S23). Because this yield exceeded the quantity expected from the amount of TBHP added on a stoichiometric basis, it indicated that the TBHP functioned as a radical initiator while the Pt_{19} SNCs provided catalytic activity during the toluene oxidation reaction at room temperature. To the best of our knowledge, this is the first report of the primary C-H bond oxidation of toluene catalyzed by heterogeneous catalysts at room temperature. The HAADF-STEM images of the subnano Pt_{19} particles after the reaction showed a relatively constant mean diameter (0.9 ± 0.2 nm), which was comparable to the size of the pristine catalyst particles. These results indicate that the dendrimer-encapsulated Pt SNCs during low-temperature oxidation retained their performance despite the leaching and aggregation of the subnano platinum particles on the carbon support.

We have demonstrated the synthesis of SNCs composed of Cu, Ru, Rh, Pd, or Pt with finely tuned sizes, using a dendrimer template. These materials showed exceptional catalytic activity during aerobic oxidation compared to available nanocatalysts. The less oxophilic Pt SNCs exhibited especially high catalytic performance and unique selectivity for useful organic compounds in the case of aerobic toluene oxidation. In particular, the Pt_{19} SNC showed the highest performance among the Pt SNCs, in agreement with results previously reported on the basis of an electrochemical study.[12c] This catalyst also demonstrated the capacity for sustained toluene oxidation at room temperature. A size-dependent oxygen activation pathway was proposed on the basis of the extended surface areas and irregular electron distributions for the SNCs, involving the formation of a hydroperoxide species on the surface via hydrogen abstraction transfer. The development of a more detailed mechanism, including theoretical considerations is currently in progress.

Acknowledgements

This study was supported by JST ERATO Grant Numbers JPMJER1503, Japan (to K.Y.) and Grant-in-Aid for Scientific Research (S), KAKENHI 15H05757 (to K.Y.). The authors also thank Dr. K. Albrecht (Tokyo Institute of Technology) for the preparation of dendrimer templates and our colleagues in the Suzukakedai Materials Analysis Division, Technical Department, Tokyo Institute of Technology, for performing ICP analyses.

Keywords: dendrimers • platinum • nanoparticles • oxidation • catalysts

References and Notes

[1] a) R. A. Sheldon, J. K. Kochi, *Metal-catalyzed oxidations of organic compounds*; Academic Press: New York, 1981; b) N. Mizuno, Ed. *Modern heterogeneous oxidation catalysis: design, reactions and characterization*; Wiley-VCH: Weinheim, **2009**.

[2] Y. Ishii, S. Sakaguchi, T. Iwahama, *Adv. Synth. Catal.* **2001** *343*, 393–427.

[3] a) E. C. Tyo, S. Vajda, *Nat. Nanotechnol.* **2015**, *10*, 577-588; b) Z. Luo, A. W. Castleman, S. N. Khanna, *Chem. Rev.* **2016**, *116*, 14456-14492; c) L. Liu, A. Corma, *Chem. Rev.* **2018**, *118*, 4981-5079.

[4] H. Guan, J. Lin, B. Qiao, X. Yang, L. Li, S. Miao, J. Liu, A. Wang, X. Wang, T. Zhang, *Angew. Chem. Int. Ed.* **2016**, *55*, 2820-2824.

[5] a) W. E. Kaden, T. Wu, W. A. Kunkel, S. L. Anderson, *Science* **2009**, *326*, 826-829; b) M. Moseler, M. Walter, B. Yoon, U. Landman, V. Habibpour, C. Harding, S. Kunz, U. Heiz, *J. Am. Chem. Soc.* **2012**, *134*, 7690-7699.

[6] a) U. Heiz, A. Sanchez, S. Abbet, W.-D. Schneider, *J. Am. Chem. Soc.* **1999**, *121*, 3214-3217; b) S. Bonanni, K. Aït-Mansour, W. Harbich, H. Brune, *J. Am. Chem. Soc.* **2014**, *136*, 8702-8707; c) J. Ke, W. Zhu, Y. Jiang, R. Si, Y.-J. Wang, S.-C. Li, C. Jin, H. Liu, W.-G. Song, C.-H. Yan, Y.-W. Zhang, *ACS Catal*. **2015**, *5*, 5164-5173.

[7] a) A. Sanchez, S. Abbet, U. Heiz, W.-D. Schneider, H. Häkkinen, R. N. Barnett, U. Landman, *J. Phys. Chem. A* **1999,** *103,* 9573-9578; b) B. Yoon, H. Häkkinen, U. Landman, A. S. Wörz, J.-M. Antonietti, S. Abbet, K. Judai, U. Heiz, *Science* **2005**, *307*, 403-407; c) A. A. Herzing, C. J. Kiely, A. F. Carley, P. Landon, G. J. Hutchings, *Science* **2008**, *321*, 1331-1335; d) Q. He, S. J. Freakley, J. K. Edwards, A. F. Carley, A. Y. Borisevich, Y. Mineo, M. Haruta, G. J. Hutchings, C. J. Kiely, *Nat. Commun.* **2016**, *7*, 12905.

[8] a) S. Vajda, M. J. Pellin, J. P. Greeley, C. L. Marshall, L. A. Curtiss, G. A. Ballentine, J. W. Elam, S. Catillon-Mucherie, P. C. Redfern, F. Mehmood, P. Zapol, *Nat. Mater.* **2009**, *8*, 213-216; b) L. Liu, U. Díaz, R. Arenal, G. Agostini, P. Concepción, A. Corma, *Nat. Mater.* **2017**, *16*, 132-139.

[9] a) D. Astruc, E. Boisselier, C. Ornelas, *Chem. Rev.* **2010**, *110*, 1857-1959; b) V. S. Myers, M. G. Weir, E. V. Carino, D. F. Yancey, S. Pande, R. M. Crooks, *Chem. Sci.* **2011**, *2*, 1632-1646; c) D. A. Tomalia, S. N. Khanna, *Chem. Rev.* **2016**, *116*, 2705-2774.

[10] S. Hecht, J. M. J. Fréchet, *Angew. Chem. Int. Ed.* **2001**, *40*, 74-91; *Angew. Chem.* **2001**, *113*, 76-94

[11] Review: K. Yamamoto, T. Imaoka, *Acc. Chem. Res.* **2014**, *47*, 1127-1136.

[12] a) K. Yamamoto, T. Imaoka, W.-J. Chun, O. Enoki, H. Katoh, M. Takenaga, A. Sonoi, *Nat. Chem.* **2009**, *1*, 397-402; b) T. Imaoka, H. Kitazawa, W.-J. Chun, S. Omura, K. Albrecht, K. Yamamoto, *J. Am. Chem. Soc.* **2013**, *135*, 13089-13095; c) T. Imaoka, H. Kitazawa, W.-J. Chun, K. Yamamoto, *Angew. Chem. Int. Ed.* **2015**, *54*, 9810-9815; *Angew. Chem.* **2015**, *127*, 9948-9953.

[13] M. Takahashi, H. Koizumi, W.-J. Chun, M. Kori, T. Imaoka, K. Yamamoto, *Sci. Adv.* **2017**, *3*, e1700101.

[14] L. Kesavan, R. Tiruvalam, M. H. Ab Rahim, M. I. bin Saiman, D. I. Enache, R. L. Jenkins, N. Dimitratos, J. A. Lopez-Sanchez, S. H. Taylor, D. W. Knight, C. J. Kiely, G. J. Hutchings, *Science* **2011**, *331*, 195-199.

[15] a) B. Fu, X. Zhu, G. Xiao, *Appl. Cat. A: Gen.* **2012**, *415-416*, 47-52; b) F. Jiang, X. Zhu, B. Fu, J. Huang, G. Xiao, *Chin. J. Cat.* **2013**, *34*, 1683-1689; c) W. Zhong, S. R. Kirk, D. Yin, Y. Li, R. Zou, L. Mao, G. Zou, *Chem. Eng. J.* **2015**, *280*, 737-747; d) X. Wang, G. Wu, H. Liu, Q. Lin, *Catalysis* **2016** *6*, 14.

[16] a) R. W. J. Scott, H. Ye, R. R. Henriquez, R. M. Crooks, *Chem. Mater.* **2003**, *15*, 3873-3878; b) R. Ye, B. Yuan, J. Zhao, W. T. Ralston, C.-Y. Wu, E. U. Barin, F. D. Toste, G. A. Somorjai, *J. Am. Chem. Soc.* **2016**, *138*, 8533-8537.

[17] Although Ru 3d photoelectrons are typically analyzed by XPS because of the strong signals, 3p spectra were used in the present work to avoid interference from carbon substrate. W. Wang, S. Guo, I. Lee, K. Ahmed, J. Zhong, Z. Favors, F. Zaera, M. Ozkan, C. S. Ozkan, *Sci. Rep.* **2014**, *4*, 4452.

[18] A small CuO cluster was reduced during XPS analyses under ultra-high vacuum. See also: C.-K. Wu, M. Yin, S. O'Brien, J. T. Koberstein, *Chem. Mater.* **2006**, *18*, 6054-6058.

[19] Y. J. Lee, E.-K. Lee, S. Kim, R. M. Nieminen, *Phys. Rev. Lett.* **2001**, *86*, 999-1002.

[20] D. M. Washecheck, E. J. Wucherer, L. F. Dahl, A. Ceriottl, G. Longoni, M. Manassero, M. Sansoni, P. Chini, *J. Am. Chem. Soc.* **1979**, *101*, 6110-6112.

[21] A. Staykov, T. Nishimi, K. Yoshizawa, T. Ishihara, *J. Phys. Chem. C* **2012**, *116*, 15992-16000.

[22] M. Boronat, A. Corma, *Dalton Trans.* **2010**, *39*, 8538-8546.

10.1002/anie.201809530

Entry for the Table of Contents

COMMUNICATION

High performance subnanocatalysis of the aerobic oxidation of toluene was achieved using dendrimer-templated metallic particles having a narrow size distribution, which promise as low-cost heterogeneous industrial catalysts. In particular, the subnano Pt_{19} particle showed the highest catalytic activity among a series of the noble metal catalysts, which was derived from the extended surface areas and the irregular electron distributions.

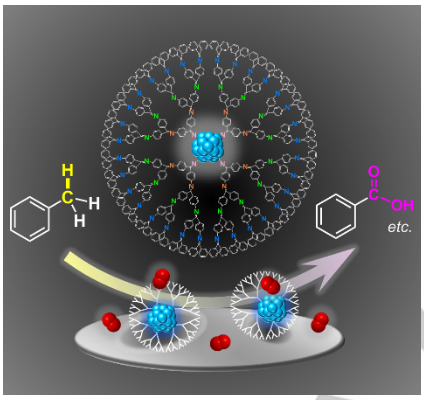

Miftakhul Huda, Keigo Minamisawa, Takamasa Tsukamoto, Makoto Tanabe, and Kimihisa Yamamoto**

Page No. – Page No.

Aerobic Toluene Oxidation Catalyzed by Subnano Metal Particles